

# Surface modification of poly(ethylene-butyl acrylate) copolymers by microwave methodology and functionalization with 4-dimethylamino-*N*-(2-hydroxyethyl)-1,8-naphthalimide for acidity sensing

S. Fernández-Alonso, T. Corrales, J.L. Pablos, F. Catalina \*

Departamento de Química Macromolecular Aplicada, Instituto de Ciencia y Tecnología de Polímeros (CSIC), C/Juan de la Cierva, 3, 28006 Madrid, Spain

## ARTICLE INFO

### Article history:

Received 28 June 2016

Received in revised form 25 August 2016

Accepted 28 August 2016

Available online 30 August 2016

### Keywords:

Surface functionalization

Microwave

Ethylene-butyl acrylate copolymers

Naphthalimide sensor

Plasma treatment

## ABSTRACT

A new procedure was developed for functionalization in the solid phase by using microwave irradiation. Heterogeneous chemical modification of poly(ethylene-butyl acrylate) copolymer (EBA), hydrolysis, chlorination, and Schotten–Baumann reactions were monitored by attenuated total reflection Fourier transform infrared (ATR-FTIR) spectroscopy. EBA was superficially functionalized by a previously synthesized fluorescent dye, 4-dimethylamino-*N*-(2-hydroxyethyl)-1,8-naphthalimide, and the depth profile of the functionalized polymer was determined by confocal Raman spectroscopy. The new functionalized materials were also evaluated as an acidic pH sensor by determining the change in the spectroscopic properties of absorption and fluorescence with pH of the solution and vapor phases. To improve the wettability of the EBA surface, oxygen plasma treatment was used and the response time of the solid sensor was analyzed.

© 2016 Elsevier B.V. All rights reserved.

## 1. Introduction

An effective approach to develop an applicable solid sensor is to modify the surface of the material that already has excellent bulk properties. A grafted surface can be produced primarily by either graft polymerization of monomers or a covalent coupling reaction of existing polymer molecules onto the substrate polymer surface. Many chemical and physical methods [1] such as plasma, e-beam, and sputtering have been used to modify the structure of polymer surfaces and in particular polyethylenes [2]. Most of these techniques are based on the use of high-energy sources that can ultimately damage the polymer surfaces either chemically or physically. Moreover, these methods are usually not versatile enough to allow the design of structurally and chemically modified surfaces through the control of the distribution of chemical functionalities throughout the surface. In an earlier work, we described the microwave-assisted chemical modification of poly(ethylene-butyl acrylate) copolymers [3] (EBA) in solution to bind coumarin derivatives through the acrylic comonomer. In this study, organic functionalities were introduced onto EBA as the polymer substrate in a controlled manner by performing a sequence of chemical reactions on the surface. In the heterogeneous phase, hydrolysis, chlorination, and Schotten–Baumann reactions were used to graft a naphthalimide derivative to

the surface of EBA. The sequence of reactions carried out is shown in Fig. 1.

The introduction of specific functional groups to polymer surfaces by well-defined, classical organic chemical reactions usually involves ionic or polar reactions rather than free radical reactions. Therefore, the polymer surfaces suitable for this type of modification must have sites that are vulnerable to electrophilic or nucleophilic attack.

The modification of the EBA surface opens the possibility to chemically bond numerous organic structures having a terminal group capable of reacting with the functional groups present on the substrate polymer surface. Recently, polymers containing photosensitive functional groups have gained significant attention [4,5,6]. A number of publications have appeared concerning 1,8-naphthalimide derivatives as a special class of environmentally sensitive fluorophores. Their strong fluorescence and good photostability have promoted their applications in a number of areas such as coloration of polymers [7,8], as laser active media [9], fluorescence markers in biology [10], anticancer agents [11], light-emitting diodes [12], photoinduced electron transfer sensors [13, 14], fluorescence switchers [15], electroluminescent materials [16,17], liquid crystal displays [18], ion probes [19], and pH sensors [20].

Hence, in this study, we synthesized a hydroxyl derivative, 4-dimethylamino-*N*-(2-hydroxyethyl)-1,8-naphthalimide (DMAN) to react with the superficial chlorine acids of the modified EBA to functionalize the polyolefin material with a sensor probe (EBA-DMAN), as shown in Fig. 1. The surface functionalization was studied by attenuated total reflection Fourier transform infrared (ATR-FTIR)

\* Corresponding author.

E-mail address: [fcatalina@ictp.csic.es](mailto:fcatalina@ictp.csic.es) (F. Catalina).

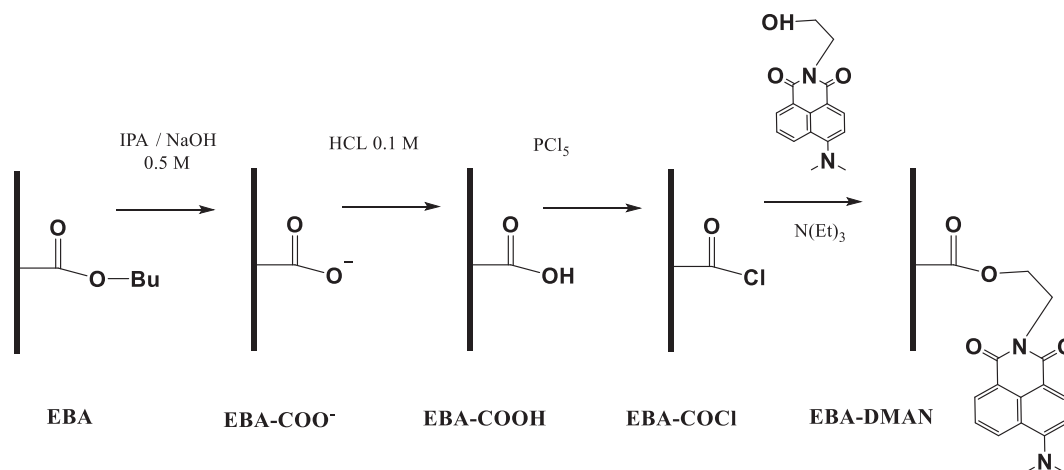


Fig. 1. Heterogeneous reaction sequence for surface modification of EBA using microwave methodology.

spectroscopy and confocal Raman spectroscopy (CRS) [21] to determine the depth profile of the functionalized polymer.

Furthermore, the new functionalized materials were evaluated as an acidic pH sensor by determining the change in the spectroscopic properties of absorption and fluorescence with pH. To improve the wettability of the surface, EBA-DMAN films were treated with oxygen plasma [22]. The plasma-treated materials (EBA-pl-DMAN) exhibited a lower response time for environmental changes of pH in solution and vapors because of surface oxidation.

## 2. Experimental

### 2.1. Materials, reagents, and film preparation

Poly(ethylene-co-butyl acrylate) copolymer (EBA) with 7% (w/w) of butyl acrylate ( $0.924 \text{ g ml}^{-1}$  of density) was supplied by Repsol company (Madrid, Spain). EBA films of  $100 \mu\text{m}$  thickness and  $50 \times 50 \text{ mm}$  dimension were prepared by compression molding in automatic Press ATLAS T8 plates with a maximum pressure of 2 tons and temperature of  $190^\circ\text{C}$ . The thickness of the films was controlled by specific-size spacer rings.

The following chemicals and solvents were purchased and used as received unless otherwise indicated: 4-bromo-1,8-naphthalic anhydride (Aldrich, 95%), 2-propanol (Scharlau, 99.5%), sodium hydroxide (Panreac, 98–100%), hydrochloric acid (VWR Chemicals, 37%), ultrapure MilliQ water (Millipore), diiodomethane (Aldrich,  $\geq 99.5\%$ ), dichloromethane (Aldrich,  $\geq 99.9\%$ ), phosphorus pentachloride (Aldrich,  $\geq 98\%$ ), triethylamine (Aldrich,  $\geq 99\%$ ), 2-aminoethanol (Aldrich, 99%), ethanol (VWR Chemicals, 99.95%), dimethylformamide (DMF, Scharlau, 99.8%), ethyl acetate (Aldrich,  $\geq 99.5\%$ ), hexane (Carlo Erba Reagents, 99%), hexadeuterated dimethylsulfoxide ( $\text{DMSO-}d_6$ , Euriso-top, 99.8%), potassium carbonate (Panreac, 99%), and coumarin 6 (Aldrich, 98%).

### 2.2. Spectroscopic characterization

ATR-FTIR was used to characterize the polymer films of EBA before and after MW reactions. ATR-FTIR spectra were obtained using a PerkinElmer BX-FTIR spectrometer coupled with a MIRacle™ ATR accessory from PIKE Technologies, and interferograms were obtained from 32 scans. The degree of hydrolysis and modifications of the EBA films were determined using ATR-FTIR and accessories with the same value of pressure.

**Confocal Raman Spectroscopy (CRS).** A Renishaw inVia Raman microscope, working in a confocal mode and connected to an Olympus BH2 microscope was used for measuring the Raman spectra. The beam from the 785 line of a He–Ne laser (laser power 320 mW at 100%) was focused by  $100\times$  magnifying length objective (numerical aperture (NA) value of 0.85) in the confocal mode and a charge-coupled device (CCD) camera as detector. Raman light was dispersed by a diffraction grating with 1200 lines/mm using a Raman holographic notch filter.

The depth profile of the sample was obtained by focusing the microscope stepwise at fixed  $1\text{-}\mu\text{m}$  intervals within the polymer film and recording 10 accumulative spectra at each step (accumulation time, 3 min per spectrum). The depth resolution of the confocal arrangement in air was previously checked using a sample of silica as a reference material.

**Ultraviolet (UV) spectroscopy** was used for the quantitative determination of DMAN moieties anchored to EBA in a PerkinElmer Lambda 35 spectrometer. DMAN surface loading was determined by measuring the absorbance at the peak maximum of absorption band. This was translated into quantitative DMAN content per unit area by rearrangement of the Beer–Lambert law. Each material was assessed in quintuplicate.

**Fluorescence spectra** were recorded using a PerkinElmer LS 55 fluorescence spectrometer. Fluorescence emission spectra of the probe were recorded in the range of 490–700 nm using the maximum of the longest-wavelength absorption band as excitation wavelength. All the spectra were corrected using the response curve of the photomultiplier. The fluorescence quantum yields ( $\Phi_F$ ) were measured relatively to coumarin 6 ( $\Phi_F = 0.78$  in ethanol) [23].

$^1\text{H}$ - and  $^{13}\text{C}$ -nuclear magnetic resonance (NMR) spectra were recorded on Varian-Mercury 400 MHz and Bruker 300 MHz NMR spectrometers using hexadeuterated dimethyl sulfoxide ( $\text{DMSO-}d_6$ ) as the solvent. Chemical shifts were reported in parts per million (ppm).  $^1\text{H}$  NMR and  $^{13}\text{C}$  NMR chemical shifts were referenced to  $\text{DMSO-}d_6$  (39.52 ppm) as standard.

Mass spectra (MS) were recorded on a HP 5973-MSD spectrometer.

### 2.3. pH measurements and spectroscopic detection of acid in solution and vapors

The pH was measured at room temperature ( $23^\circ\text{C}$ ) by using a Mettler Toledo SevenGo Duo pro meter with an InLab Expert Pro ISM-ID67 electrode that was previously calibrated with standard buffers. The sensing measurements of the solutions of DMAN and surface-modified films of EBA-DMAN were performed using HCl solution in the water:ethanol (4:1) mixture as solvent.

Acid titration by ultraviolet–visible (UV–Vis) and fluorescence spectrometry in aqueous solution and vapors was performed as follows. The titration of the solution with DMAN (water:ethanol 4:1,  $10^{-4}$  M) was carried out by adding dilute HCl to increase the acidity from pH 8 to pH 0.5. After each addition, the solutions were allowed to equilibrate for 10 min, the pH was measured, and UV–Vis and fluorescence spectra were recorded.

In the case of functionalized materials (EBA-DMAN and EBA-pl-DMAN), the films were cut into strips of dimension  $1 \times 4$  cm and dipped into 100 ml of water (Millipore-Q) using a homemade support that is slotted into the cell holder of the spectrophotometers. To study the effect of increasing the acidity of the medium beyond the pH scale, vials containing 50 ml of HCl at pH 7 to  $-1.1$  (12 M HCl, 37%) were prepared. Strips of the film were immersed in these vials, starting from the vial with the lowest acid concentration, and the UV–Vis and fluorescence spectra were recorded for each pH after a conditioning time of 2 h. The fluorescence detection of acidic vapors was performed by adding 100  $\mu$ l of HCl (12 M HCl 37%) over a cotton fragment to avoid direct contact and placing it at the bottom of a sealed spectrophotometric cuvette, where the functionalized EBA film is disposed.

#### 2.4. Microwave equipment

The microwave equipment used in this study was an Anton Paar Monowave™ 300 microwave synthesis reactor equipped with an infrared sensor (IR pyrometer). All reactions were performed in pressure-resistant 30-ml test tubes sealed with silicon septum with a magnetic stirring bar. The progress of the reactions was observed by an integrated CCD camera, which directly focuses on the reaction vial.

#### 2.5. Plasma treatment and characterization by contact angle measurements and atomic force microscopy

The films were plasma-treated using an RF-Expanded Plasma Cleaner PDC-002 coupled with a PlasmaFlo PDC-FMG gas mixer obtained from Harrick Plasma and a Varian SH-110 vacuum pump. Samples were placed inside the Pyrex chamber (6" diameter  $\times$  6.52" length), and both sides of all films were treated with high RF power (30 W to the RF coil) for 30 min with oxygen plasma. Gas flow rates and chamber pressure can be altered by manual pressure and flow regulators, and stabilized pressure was fixed at 250 mTorr (0.33 mbar).

Changes in the wettability of plasma-treated polymer surfaces were observed after the determination of water contact angle (CA) by the sessile drop method. CA measurements were performed at 25 °C using a KSV instruments LTD CAM 200 Tensiometer and MilliQ water as wetting solvent. Surface energy was determined using two liquids (water and methylene iodide) for the measurements. On the basis of Owens-Wendt's method [24], the surface energy ( $\gamma$ ) and its dispersive ( $\gamma^d$ ) and polar ( $\gamma^p$ ) parts were calculated using the CAM 200 software.

Surface morphology and roughness of the EBA films modified with DMAN before and after oxygen plasma treatment were examined by atomic force microscopy (AFM) using a Nanoscope IV system (Digital Instruments) working in tapping mode with a triangular microfabricated cantilever having a length of 115–135 nm, 1- to 10-Ohm-cm phosphorous (n)-doped Si pyramidal tip, and a nominal spring constant of 20–80 N m $^{-1}$ . The mean roughness value (Ra) represents the arithmetic average of the deviations from the center plane of the sample, which was determined using standard Digital Instruments software.

#### 2.6. Surface modification of EBA films by hydrolysis (EBA-COOH) and acid chlorination (EBA-COCl)

EBA (7% of BA) film was cut into strips ( $1 \times 4$  cm) and hydrolyzed in the solid state by a modified procedure of the method reported previously [3] to conduct the heterogeneous reaction in a microwave reactor.

The EBA film was placed in a 30-ml microwave test tube, and the test tube was then filled with a solution of 0.5 M NaOH in isopropanol. The temperature of the solution was fixed at 65 °C under stirring at 600 rpm for 6 h. After completion of the heterogeneous reaction at room temperature, the EBA-COO $^{-}$  film was separated from the medium and neutralized in a microwave-assisted second step by adding 30 ml of aqueous HCl solution (0.1 M) to the polymer and maintaining the mixture at 50 °C for 1 h. The resulting hydrolyzed EBA-COOH film was then washed repeatedly with distilled water and dried under vacuum overnight. The surface modification of EBA to EBA-COO $^{-}$  and EBA-COOH was confirmed and evaluated by ATR-FTIR spectroscopy (Fig. 3).

The EBA-COOH film and phosphorus pentachloride (50 mg, 0.24 mmol) were placed in a 30-ml microwave reactor containing 20 ml of CH $_2$ Cl $_2$  anhydrous solution. Acid chlorination was carried out under microwave irradiation at 55 °C under magnetic stirring at 600 rpm. After 90 min, the EBA-COCl film was washed with dichloromethane and dried under vacuum overnight. The reaction between superficial acid groups and EBA-COCl was quantitative and confirmed by ATR-FTIR spectroscopy (Fig. 3).

#### 2.7. Functionalization of EBA-COCl with DMAN

Superficially chlorinated EBA film, EBA-COCl, and 25 mg of DMAN were placed in a vial containing 20 ml of CH $_2$ Cl $_2$  and 500  $\mu$ l of triethylamine (TEA) under microwave at 55 °C for 15 h under magnetic stirring at 600 rpm. The vial was then rapidly cooled down with compressed air to room temperature, and the modified EBA-DMAN film was washed repeatedly with dichloromethane and dried under vacuum overnight. The reaction was confirmed by ATR-FTIR and UV–Vis spectroscopy (Fig. 3).

#### 2.8. Synthesis of N-(2-hydroxyethyl)-4-dimethylamino-1,8-naphthalimide

N-(2-hydroxyethyl)-4-bromo-1,8-naphthalimide (compound 1) and N-(2-hydroxyethyl)-4-dimethylamino-1,8-naphthalimide (compound 2) were synthesized following the procedure (Fig. 2) described in refs. [25,26] and using a novel reaction [27] for dimethylation of compound 1.

In a pressure-resistant microwave test tube, a mixture of 4-bromo-1,8-naphthalic anhydride (1.4 g, 0.005 mol) and ethanol amine (0.4 g, 0.005 mol) in ethanol (15 ml) was heated at 85 °C and stirred at 600 rpm for 2 h. The resulting mixture was cooled at 5 °C. The solid product obtained was filtered and washed with 30 ml of cold ethanol thrice and then identified as N-hydroxyethyl-4-bromo-1,8-naphthalimide (compound 1) after drying. Yield 90% (1.4 g). M.p.:  $206 \pm 2^\circ$ .  $^1\text{H}$  NMR ( $\delta_{\text{H}}$  ppm) (300 MHz, DMSO- $d_6$ , Me $_4$ Si):  $\delta$  8.42 (dd,  $J = 13.9, 7.9$  Hz, 2H), 8.20 (d,  $J = 7.9$  Hz, 1H), 8.10 (d,  $J = 7.8$  Hz, 1H), 7.89 (t,  $J = 7.9$  Hz, 1H), 4.81 (s, 1H), 4.10 (t,  $J = 6.4$  Hz, 2H), 3.61 (t,  $J = 5.9$  Hz, 2H).  $^{13}\text{C}$  NMR ( $\delta_{\text{C}}$  ppm) (100.6 MHz, DMSO- $d_6$ , Me $_4$ Si):  $\delta$  162.90, 162.85, 132.41, 131.42, 131.24, 130.80, 129.61, 128.98, 128.67, 128.14, 122.70, 121.92, 57.71, 41.95. FTIR (wavenumbers, cm $^{-1}$ ):  $\nu_{\text{OH}}$  3386 cm $^{-1}$ ;  $\nu_{\text{C-H}}$  3066 cm $^{-1}$  aromatic stretch vibration;  $\nu_{\text{C=O}}$  1692, 1658 cm $^{-1}$ ;  $\nu_{\text{N-C=O}}$  1611 cm $^{-1}$ ;  $\nu_{\text{C-C}}$  1585, 1568 cm $^{-1}$  aromatic ring chain vibrations. Elemental analysis, theoretical values: %C 52.52; %H 3.15; %N 4.38; experimental values: %C 52.42; %H 3.25; %N 4.25; EI-MS  $m/z$ : 321.0 (M $^{+}$ ).

In a pressure-resistant microwave test tube, 1 g of compound 1 (0.003 mol), 4.35 ml of triethylamine (0.03 mol), and 10 ml of DMF:water (1:1) solution were added. The mixture was heated at 120 °C and stirred at 600 rpm for 12 h. After completion of the reaction, the vial was cooled with water to room temperature. The mixture was extracted with ethyl acetate ( $4 \times 50$  ml), and the organic layer was dried over K $_2$ CO $_3$ . The solvent was evaporated under reduced pressure, which was purified by silica gel column chromatography using ethyl acetate:hexane (2:1) as eluent to obtain an orange solid product, which is identified as N-(2-hydroxyethyl)-4-dimethylamino-1,8-

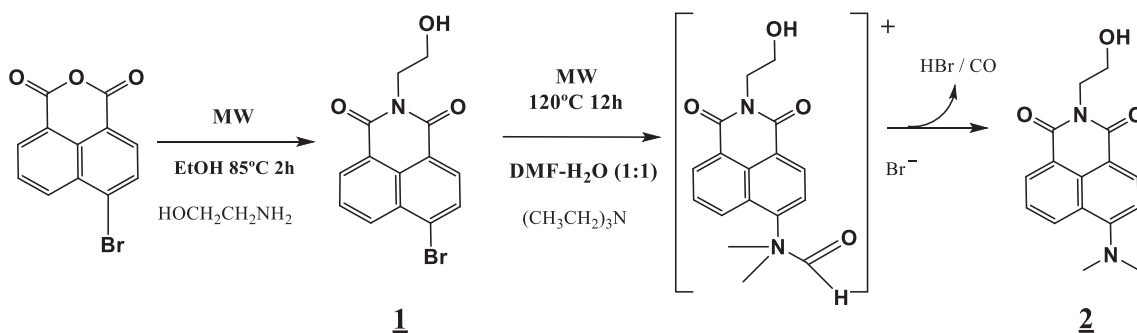


Fig. 2. Reaction pathway and mechanism for the synthesis of *N*-(2-hydroxyethyl)-4-dimethylamino-1,8-naphthalimide (DMAN, compound 2).

naphthalimide. Yield: 84%, M.p. =  $135 \pm 2$  °C.  $^1\text{H}$  NMR ( $\delta_{\text{H}}$  ppm) (400 MHz, DMSO- $d_6$ , Me $_4$ Si):  $\delta$  8.51 (dd,  $J = 8.5, 1.1$  Hz, 1H), 8.45 (dd,  $J = 7.3, 1.1$  Hz, 1H), 8.34 (d,  $J = 8.3$  Hz, 1H), 7.75 (dd,  $J = 8.5, 7.3$  Hz, 1H), 7.21 (d,  $J = 8.3$  Hz, 1H), 4.81 (t,  $J = 6.0$  Hz, 1H), 4.13 (t,  $J = 6.6$  Hz, 2H), 3.59 (q,  $J = 6.5$  Hz, 2H), 3.08 (s, 6H).  $^{13}\text{C}$  NMR ( $\delta_{\text{C}}$  ppm) (100.6 MHz, DMSO- $d_6$ , Me $_4$ Si):  $\delta$  163.69, 163.03, 156.41, 132.12, 131.32, 130.41, 129.56, 124.90, 124.16, 122.37, 113.43, 112.91, 57.87, 44.35, 41.51. FTIR (wavenumbers,  $\text{cm}^{-1}$ ):  $\nu_{\text{OH}}$  3474  $\text{cm}^{-1}$ ;  $\nu_{\text{C=O}}$  1680  $\text{cm}^{-1}$  and 1628  $\text{cm}^{-1}$ ,  $\nu_{\text{C-C}}$  1575  $\text{cm}^{-1}$  aromatic ring chain vibrations. Elemental analysis, theoretical value: %C 67.59; %H 5.67; %N 9.85; experimental values: %C 67.09; %H 5.88; %N 9.88. EI-MS  $m/z$ : 285.0 ( $\text{M}^+$ ).

### 3. Result and discussion

#### 3.1. Synthesis of *N*-(2-hydroxyethyl)-4-dimethylamino-1,8-naphthalimide

The synthesis route to obtain *N*-(2-hydroxyethyl)-4-dimethylamino-1,8-naphthalimide is presented in Fig. 2. In the first step, the condensation of 4-bromo-1,8-naphthalic anhydride with 2-hydroxyethylamine under microwave irradiation in ethanol at 85 °C afforded compound 1 in high yield at a shorter reaction time than conventional conditions. It has been observed [28] that for various amines, imidation of naphthalimides under reflux required 4–16 h. Our results show that the microwave method reduced the reaction time and improved the yield from 72–85% (under conventional conditions) to 96%.

In the second reaction step (Fig. 2), an interesting observation was made while we were optimizing the reaction conditions for the nucleophilic substitution reaction of compound 1 with 2-methoxyethylamine. When the reaction was carried out in DMF, surprisingly, dimethylamination product (DMAN, compound 2) was also produced. In the absence of the primary amine, DMAN was obtained in very good yield. This reaction has been described [27,29] as a convenient method for the introduction of a dimethylamino group in aromatic compounds through chlorinated derivatives of heterocycles or aromatics using bases such as KOH or  $\text{K}_2\text{CO}_3$ , and although the reaction mostly proceeds slowly, it results in good yields.

In our experimental conditions, dimethylamination resulted in the formation of compound 2 in good yield. On the contrary, when no base was added, the reaction did not proceed. Also, the presence of water seemed to be crucial for the amination, and this fact could be attributed to a better solvation of the base. The reaction and the plausible mechanisms for the amination are illustrated in Fig. 2.

The reaction starts with a base-assisted cleavage of DMF to form the required dimethylamine [30,31], which acts as the nucleophile for the formation of the required product. DMF is an easy substitute for dimethylamine, and the reaction occurs in a shorter period of time and produces high yields with microwave irradiation. The best conditions were noted under microwave irradiation for 12 h at 850 W and a ceiling temperature of 120 °C of a mixture of compound 1 together

with 10 equiv. of triethylamine in DMF:water (1:1) yielding compound 2 in 90%.

#### 3.2. Microwave-assisted surface hydrolysis, acid chlorination, and functionalization of EBA with naphthalimide groups

The functionalization of EBA (7% content of BA) was carried out following the sequence of reactions shown in Fig. 1. The different modifications of EBA, hydrolysis of butyl ester, acid chlorination, and esterification with DMAN were accomplished successfully in solution under microwave irradiation. All the modified EBA films were isolated and characterized by ATR-FTIR spectroscopy (Fig. 3).

Fig. 3 shows the characteristics of vibrational bands of the species formed after each functionalization step as described above in the synthesis section. As shown in Fig. 3, butyl ester on the surface was hydrolyzed by microwave irradiation under heterogeneous conditions, and the degree of hydrolysis was determined by ATR-FTIR as described earlier [3] and by using the butyl ester and carboxylate bands. The obtained curves are plotted in Fig. 4.

The spectra at different hydrolysis reaction times show the growth of bands because of the increase in carboxylate content, introduced to the surface of the polyolefin film. This confirms the hydrolysis of the surface with treatment time. Thus, the carboxylate content can be used to follow the modification of EBA surface by ATR-FTIR.

After reacting sodium hydroxide solution (0.5 M) in isopropanol for 6 h at 65 °C, the conversion of butyl ester to carboxylate (Fig. 4) reaches a value of 83.3% (5.83% of butyl ester content). In our experimental condition, 1.17% of butyl ester remained in the EBA composition after hydrolysis in the superficial thickness of the film analyzed by ATR-FTIR. As found in the hydrolysis reactions carried out in bulk with EBA [3] and ethylene vinyl acetate (EVA) copolymers [32], a plateau was reached in the hydrolysis conversion when the reaction times are longer than 6 h.

The determination of the acid content by ATR-FTIR suggested the carboxylic acid band at 1703  $\text{cm}^{-1}$  is attributed to the overlapping of the carbonyl butyl ester band at 1735  $\text{cm}^{-1}$ . The asymmetric stretch band of the carboxylate group at 1580  $\text{cm}^{-1}$  could therefore be more convenient to follow the hydrolysis conversion.

After protonation of the carboxylate groups in a microwave-assisted second step (HCl aq. solution 0.1 M, 50 °C, 1 h), the acid groups present in EBA-COOH were converted to acid chloride under microwave heating. After 1.5 h of reaction with phosphorus pentachloride, the transformation was quantitative, as shown by the band at 1793  $\text{cm}^{-1}$ , which corresponds to  $\nu_{\text{C=O}}$  acyl chloride (EBA-COCl) and the disappearance of the acid band at 1703  $\text{cm}^{-1}$  (Fig. 3).

Finally, functionalization was carried out by reacting EBA-COCl with the previously obtained *N*-(2-hydroxyethyl)-4-dimethylamino-1,8-naphthalimide derivative. The degree of functionalization increased with reaction time (3 h: 45%; 5 h: 60%; 7 h: 70%; and 10 h: 83%). After reacting for 15 h at 55 °C, no acyl halide band in the functionalized EBA-DMAN film could be detected at 1793  $\text{cm}^{-1}$ , suggesting that the



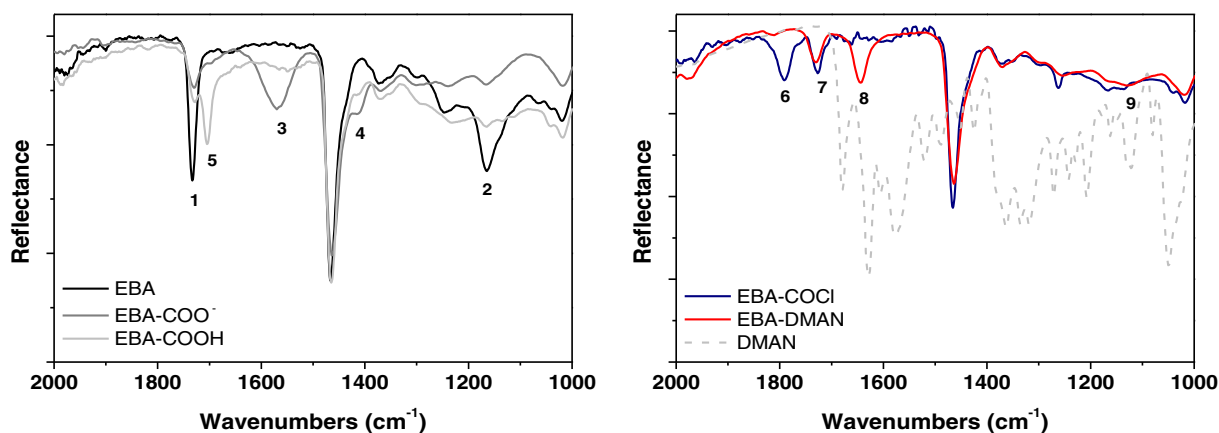


**Fig. 3.** ATR-FTIR spectra in the region between 2000 and 1000  $\text{cm}^{-1}$  of EBA (7% of BA content) and the surface-modified EBA materials: (1) 1735  $\text{cm}^{-1}$   $\nu_{(\text{C}=\text{O})}$  butyl ester (EBA), (2) 1165  $\text{cm}^{-1}$   $\nu_{(\text{C}-\text{O})}$  aliphatic ester (EBA), (3) 1568  $\text{cm}^{-1}$  and (4) 1413  $\text{cm}^{-1}$  are assigned to  $\nu_{\text{as}(\text{COO}^-)}$  and  $\nu_{\text{s}(\text{COO}^-)}$  of carboxylate anion, respectively, (EBA- $\text{COO}^-$ ), (5) 1703  $\text{cm}^{-1}$   $\nu_{(\text{C}=\text{O})}$  carboxylic acid (EBA- $\text{COOH}$ ), (6) 1793  $\text{cm}^{-1}$   $\nu_{(\text{C}=\text{O})}$  acyl chloride (EBA- $\text{COCl}$ ), (7) 1730  $\text{cm}^{-1}$   $\nu_{(\text{C}=\text{O})}$  naphthalimide (EBA-DMAN), (8) 1644  $\text{cm}^{-1}$   $\nu_{(\text{C}=\text{C})}$  naphthalimide aromatic ring (EBA-DMAN), and (9) 1167  $\text{cm}^{-1}$   $\nu_{(\text{C}-\text{O})}$  aliphatic ester (EBA-DMAN).

reaction was quantitative and the content of naphthalimide on the surface remained constant after several washes with dichloromethane.

The amount of naphthalimide superficially bonded to the EBA was determined spectrophotometrically through the measurement of absorbance at the peak maximum of the absorption band and using the absorption coefficient of *N*-(2-hydroxyethyl)-4-dimethylamino-1,8-naphthalimide in water:ethanol (4:1 w/w) ( $\epsilon_{445} = 1.02 \times 10^4 \text{ mol}^{-1} \text{ l cm}^{-1}$ ). Analysis of EBA-DMAN by UV spectroscopy provided a measure of the surface content of DMAN per unit area of polymer, and a concentration value of  $2.4 \pm 0.20 \mu\text{g cm}^{-2}$  was calculated for the EBA-DMAN film hydrolyzed after 6 h. For the materials with a lower initial degree of hydrolysis, a good correlation was observed between increasing the extent of acid chlorination on EBA and increased content of DMAN bonded to the EBA.

### 3.3. Depth profiling of the functionalization by CRS

Chemical functionalization of EBA-DMAN polymer films was studied using Raman microscopy. Both physical and chemical surface modification reactions generally result in the formation of a concentration gradient of the modifying groups through the film, and we used CRS to characterize the depth profile [33] of DMAN anchored to the EBA-DMAN films.

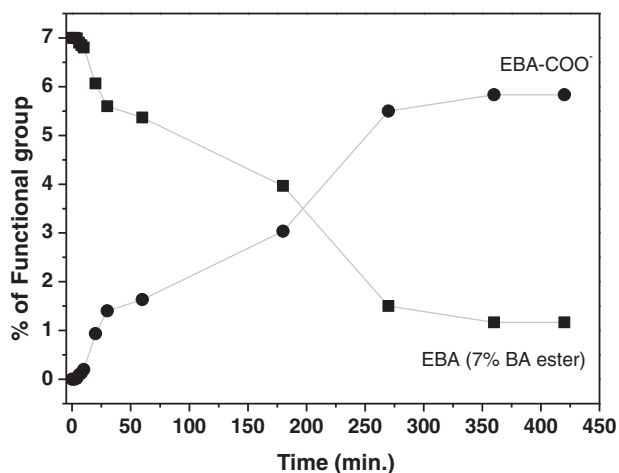


**Fig. 4.** Relationship between the percentages of surface hydrolysis degree of butyl ester (■) and carboxylate formation (●) and reaction time in EBA films (7% content in BA) determined from the ATR-FTIR spectra.

To obtain the depth profile of the films, a Raman microscope was focused stepwise (1  $\mu\text{m}$ ) from near the surface down to the center of each film, and the 1000- to 1800- $\text{cm}^{-1}$  region of the spectrum was recorded at each step. In addition to the typical EBA polymer peaks, new characteristic bands emerged for graphitic material EBA-DMAN.

The degree of modification as a function of depth was obtained from the relative intensity of the naphthalimide bands and  $\nu_{(\text{C}-\text{C})}$  aromatic ring vibrations at 1585  $\text{cm}^{-1}$  with respect to the  $\nu_{(\text{C}-\text{C})}$  aliphatic chain vibrations of the EBA at 1296  $\text{cm}^{-1}$ . Hence, signals  $[I(1585 \text{ cm}^{-1})/I(1296 \text{ cm}^{-1})]$  lead to the relative depth profile, which is depicted in Fig. 5.

The shape of the curve shown in Fig. 5 confirms that the EBA has not only been modified at the surface, but a gradient of DMAN was also formed across the first 20  $\mu\text{m}$  of film thickness until the naphthalimide Raman bands are negligible. Relative degrees of hydrolysis of the EBA and the subsequent functionalization are a function of the depth without any interface between the pure EBA layers and functionalized layers. This behavior has been described by other authors using this technique to modify polyvinyl chloride (PVC) [34] and in the nitration of polystyrene [35] without any swelling of the polystyrene film. In our reaction conditions of hydrolysis (6 h at 65  $^{\circ}\text{C}$  using 0.5 M NaOH in isopropanol),

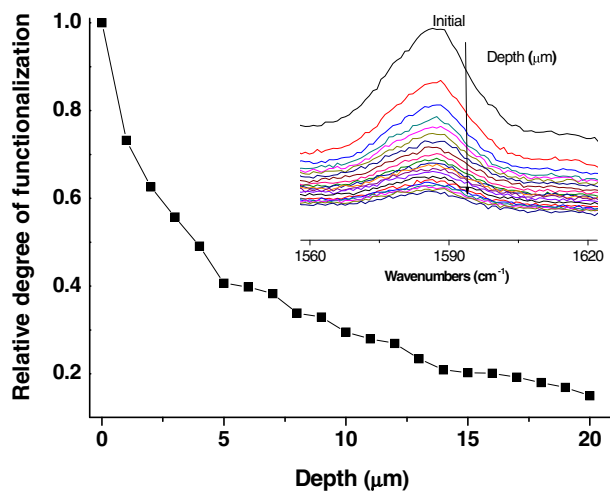


**Fig. 5.** Relative depth profile of functionalization calculated from the evolution of the Raman band  $\nu_{(\text{C}-\text{C})}$  aromatic ring vibrations of naphthalimide at 1585  $\text{cm}^{-1}$  (inset) versus depth. Spectra of a functionalized EBA-DMAN film (100  $\mu\text{m}$ ) were recorded using confocal Raman spectroscopy and normalized with respect to the intensity of the  $\nu_{(\text{C}-\text{C})}$  band at 1296  $\text{cm}^{-1}$  of the aliphatic chain vibrations of the EBA.

the polyolefin film did not swell, and hence, the extent of hydrolysis (83.3% of butyl ester content of EBA) is confined to the first 20  $\mu\text{m}$  from the surface down to the film center as the DMAN depth profile.

CRS is a useful technique to measure the functionalization of polymer surface through the depth profile using Raman absorption band characteristics of the anchored functionalities.

### 3.4. Effect of pH on the absorption and fluorescence properties of DMAN and EBA-DMAN

Light excitation of DMAN elicits an electron donor–acceptor interaction between the unbound electron pair of the nitrogen atom at C-4 position toward the electron-accepting *peri*-carboximide groups [36,37]. This intramolecular electron charge transfer (ICT) results in a long-wavelength broad absorption band with absorption maxima at 445 and 402 nm for DMAN (Fig. 6A) and EBA-DMAN (Fig. 6B), respectively. Upon acidification, the maximum intensity of the band decreases from pH approximately 3 to 0 (Fig. 6C). When the aromatic amine of the naphthalimide derivative is protonated at low pH values, the electron-withdrawing effect leads to fluorescence quenching (Fig. 6D). This effect can also be observed for the DMAN bonded to the surface of EBA (Fig. 6B). The effect of pH on the absorbance and fluorescence of DMAN and EBA-DMAN is illustrated in Fig. 6.

For EBA-DMAN, the decrease in absorbance and the corresponding quenching of fluorescence due to the amine protonation occurs at lower pH values than that obtained for DMAN (Fig. 6C and F). This fact could be due to the hydrophobic characteristic of the EBA surface. Hence, EBA-DMAN films were used to evaluate the molarity of HCl aqueous solutions in the interval of 1–12 M with the change in absorbance (Fig. 6B) and fluorescence (Fig. 6E) characteristics as a function of pH [38]. Table 1 summarizes some spectroscopic parameters obtained from the spectra.

When the DMAN chromophore is bonded to the EBA through the 2-hydroxyethyl group, the absorption and fluorescence maxima exhibit a

**Table 1**

Parameters for *N*-(2-hydroxyethyl)-4-dimethylamino-1,8-naphthalimide (DMAN) in solution and bonded to the polymer film (EBA-DMAN) determined according to pH dependence by UV–Vis absorption and fluorescence spectroscopy<sup>(a)</sup>.

Parameter	DMAN	EBA-DMAN
$\lambda_{\text{ABS-acid}}$	332, 346 nm	327, 348 nm
$\text{Log } \epsilon_{\text{acid}}^{(b)}$	4.08 (332 nm)/4.05 (346 nm)	—
$\lambda_{\text{Isobestic}}$	305, 360 nm	370 nm
$\lambda_{\text{ABS-base}}$	445 nm	402 nm
$\text{Log } \epsilon_{\text{base}}^{(b)}$	4.01 (445 nm)	—
$\text{pK}_a^{(c)}$	1.41	—0.88
$\lambda_{\text{FLU-acid}}$	548 nm	480 nm
$\lambda_{\text{FLU-base}}$	550 nm	488 nm
$\Phi_{\text{FLU-solvent}}^{(f)}$	0.032 (water:ethanol, 4:1, v/v)	water:ethanol (4:1, v/v) << ethanol << hexane
	0.85 (ethanol)	
	0.85 (hexane)	
$\Delta\nu^{(g)}$	4290.1	4425.7

<sup>a</sup> Measured at  $10^{-4}$  M in water:ethanol (4:1, v/v). The subscripts “acid” and “base” refer to the limiting value of a given parameter when the acid or base condition is increased, respectively. Fluorescence emission spectra were obtained by excitation at  $\lambda_{\text{MAX}}$ .

<sup>b</sup>  $\epsilon$ , molar absorptivity in  $\text{M}^{-1} \text{cm}^{-1}$ .

<sup>c</sup> Obtained [37] by analyzing the pH dependence of the absorbance ( $A$ ) at a given wavelength according to the equation  $\log[(A_{\text{acid}} - A)/(A - A_{\text{base}})] = \text{pH} - \text{pK}_a$ .

<sup>f</sup> Relatively to coumarin 6 ( $\Phi_F = 0.78$  in ethanol).

<sup>g</sup> Stokes shift ( $\nu_{\text{FLU}} - \nu_{\text{ABS}}$ ) in frequency ( $\text{cm}^{-1}$ ).

marked hypsochromic shift of 40–60 nm without a decrease in intensity and maintaining the Stokes shift (Table 1). The fluorescence quantum yield of DMAN is low in polar and base–neutral media, but is drastically increased to 0.85 in hexane. These results are in agreement with those obtained by other authors [37] for *N*-methyl-4-dimethylamino-1,8-naphthalimide. The corresponding fluorescence quantum yields of EBA-DMAN were not determined because of difference between the functionalized film and the fluorescence standard used in solution, but the relative fluorescence intensities of EBA-DMAN were in the same intensity order: water:ethanol (4:1, v/v) << ethanol << hexane.

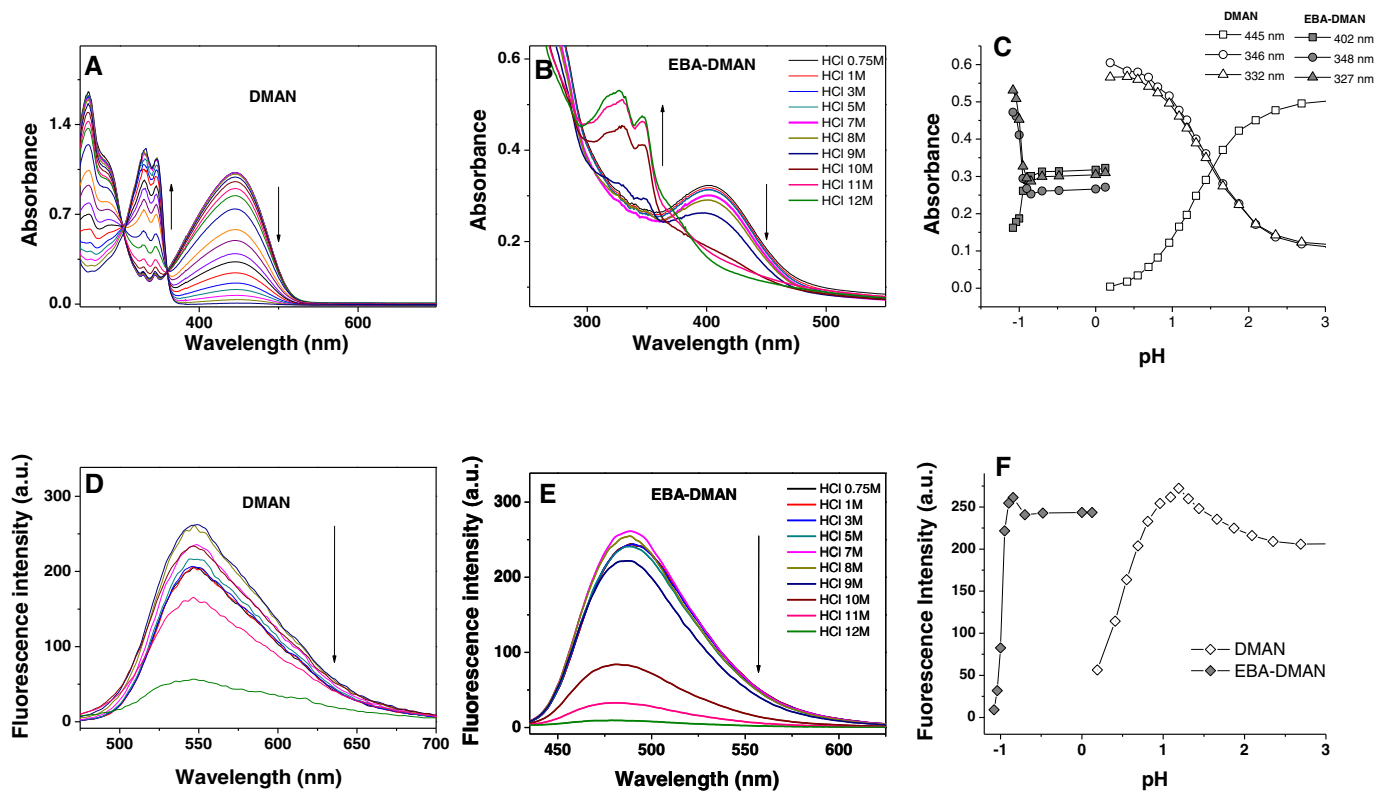


**Fig. 6.** Spectroscopic characteristics as a function of pH of acid media: Absorption of DMAN (A) and EBA-DMAN (B) and fluorescence of DMAN (D) and EBA-DMAN (E). Comparison of the absorption (C) and fluorescence (F) changes with pH for DMAN and EBA-DMAN.

The  $pK_a$  of EBA-DMAN has a negative value ( $-0.88$ ) and is lower than that of DMAN ( $1.41$ ), as the dimethylamine protonation of EBA-DMAN occurs at lower pH than that observed for DMAN (Fig. 6).

The EBA-DMAN material acts as an extreme acidity sensor by its absorbance and fluorescence characteristics. The sensor activity of EBA-DMAN was effective under several acid–water wash cycles (until 4–5 cycles), but with a prolonged response time ( $\sim 2$  h). Also, reversibility was observed with lower recovery of the fluorescence after the fourth cycle. One possibility to decrease the response time to acid media is to increase the hydrophilicity of the EBA surface through oxygen plasma treatment. In the next section, we report the results obtained from EBA-DMAN before and after plasma treatment as a sensor of acidity.

### 3.5. Plasma treatment of EBA-DMAN films and characterization

To enhance the hydrophilic characteristic of the functionalized EBA, the EBA-DMAN films were exposed to oxygen plasma for 30 min. Plasma treatment causes cleavage of macromolecular chains, generation of free radicals and oxygen-containing functionalities, and subsequent rearrangement of modified chains [39]. Plasma treatment can induce several surface changes [40], with serious impacts on consequent applications such as alterations in biocompatibility and antibacterial properties [41].

These processes have a significant effect on surface wettability. The content of DMAN bonded to the polymer remained constant after the treatment, but important changes were observed in the water CA. The obtained results are summarized in Table 2.

The plasma-treated film EBA-pl-DMAN exhibited a hydrophilic characteristic because of the presence of oxidative species on the surface [42]. The value of the water CA of EBA (7% BA),  $106.5^\circ$ , changed to  $92.6^\circ$  for EBA-DMAN, and after 30 min of treatment with oxygen plasma (EBA-pl-DMAN), this value further decreased to  $41^\circ$ . The measured CAs were then used to calculate the polar, disperse, and total surface energies of the modified EBA films. The change in the total surface energy ( $\gamma$ ) and its polar ( $\gamma^p$ ) and dispersive ( $\gamma^d$ ) components of the modified EBA films was calculated by Owens–Wendt's method. The variation in the values of the total, polar, and disperse solid surface energies (Table 2) of EBA-DMAN before and after oxygen plasma treatment, EBA-pl-DMAN, shows that the total surface energy of EBA-DMAN increases from  $30.91 \text{ mN m}^{-1}$  for untreated film to  $62.39 \text{ mN m}^{-1}$  for oxygen plasma-treated film EBA-pl-DMAN. Compared with the untreated film, plasma-treated films have higher total surface energy, particularly for the polar component.

The change in EBA-DMAN surface structure and the topography after oxygen plasma modification were imaged and measured by AFM. The AFM images of the untreated and oxygen plasma-treated films are presented in Fig. 7.

The average roughness ( $R_a$ ) of untreated films was  $12.5 \text{ nm}$ , and their surface pattern was relatively smooth. After 30 min of oxygen plasma treatment, the treated EBA-pl-DMAN exhibited high density of height features distributed on the surface (Fig. 7). As expected, the average roughness was increased to  $35.5 \text{ nm}$ . The mean surface roughness of EBA-pl-DMAN was increased by approximately three times, confirming

that the change in morphology is the result of the ion bombardment and ablation of the polymer surface layer.

### 3.6. Plasma treatment of EBA-DMAN films and response time to acid media

The changes in fluorescence emission with HCl (37%, 12 M) as a function of time are shown in Fig. 8A and B for EBA-DMAN and EBA-pl-DMAN, respectively.

The oxygen plasma treatment substantially decreased the response time of the DMAN fluorescence in strong acid medium (HCl, 12 M) from 80 min for EBA-DMAN to 30 min for EBA-pl-DMAN (Fig. 8C), together with a larger decay of fluorescence in the plasma-treated film. The increase in hydrophilicity imparted by the oxidative plasma on the film surface facilitates the penetration of proton into the coordination sphere of the DMAN functional groups anchored to the first  $20 \mu\text{m}$  of the film. The remaining nonprotonated DMAN chromophore after acid treatment was higher for the EBA-DMAN film, as the residual fluorescence intensity is stronger than that observed for the EBA-pl-DMAN film. This fact confirms a deeper penetration of protons into the plasma treatment material. Also, the reversibility of dimethylamine protonation after washing with water was compared for both materials. Again, the extent of deprotonation is lower for EBA-DMAN (Fig. 8D), as the fluorescence intensity of EBA-pl-DMAN (Fig. 8E) was totally recovered after washing with distilled water. Thus, oxygen plasma treatment improved the sensitivity of the functionalized EBA surface to the acid medium.

The response time of functionalized films to the extremely acidic environment was also studied in the vapor phase, it was observed that the spectroscopic characteristics of DMAN bonded to the polymer were sensitive to the acid vapor medium. It was necessary to maintain the film for approximately 1 h to observe the effective change in absorption and fluorescence properties. The results are shown in Fig. 9.

Both functionalized materials are sensitive to HCl vapors through their ICT absorption bands at the longest wavelength (Fig. 9A and B). The plasma-treated EBA-pl-DMAN film exhibits better behavior in fluorescence decay after 120 min of vapor treatment (Fig. 9D) than the untreated EBA-DMAN film (Fig. 9C). The vapor penetration into the surface materials was improved by the surface oxidation induced by the plasma.

The hydrophilicity of the EBA surface clearly improved the sensor activity of the DMAN chromophore bonded to the surface.

In this study, we have described a useful procedure to modify and functionalize the polyolefin copolymer EBA, thereby opening the possibility of anchoring numerous interesting structures containing functionalities capable of reaction with acid chlorine groups introduced by microwave irradiation. The functionalized surface films of EBA-DMAN act as strong acid sensors in both solution and vapor phases. The post-functionalization treatment with oxygen plasma decreased the response time to the acid media and increased the penetration of protons into the material. This functionalization with dimethylamine naphthalimide derivatives such as those used in this study or other fluorescence probes could result in a variety of film sensors of significant interest in environmental applications.

## 4. Conclusions

In conclusion, we have demonstrated that microwave irradiation allows rapid and efficient attachment of hydroxyl naphthalimide functionalities to superficially acid-chlorinated ethylene-butyl acrylate copolymers (EBA-COCl). The previous modifications of EBA (7% of BA) films (hydrolysis and acid chlorination) occur efficiently in a heterogeneous phase under our experimental conditions.

CRS was a useful technique to measure the functionalization of the polymer surface through the depth profile, and the results demonstrated that the heterogeneous modification was confined to the first  $20 \mu\text{m}$  from the surface down to the film center.

**Table 2**

Contact angle (CA) and total ( $\gamma$ ), polar ( $\gamma^p$ ), and disperse ( $\gamma^d$ ) surface energy data for EBA (7% of BA content) and the surface-modified EBA materials.

	Static CA ( $^\circ$ )		Surface energy ( $\text{mN m}^{-1}$ ) <sup>a</sup>		
	Water	Diiodomethane	$\gamma$	$\gamma^p$	$\gamma^d$
EBA	106.5	55.0	29.38	0.38	29.00
EBA-COOH	85.9	66.6	29.51	4.99	24.53
EBA-DMAN	92.6	60.8	30.91	2.33	28.58
EBA-pl-DMAN	41.0	51.5	62.39	28.44	33.95

<sup>a</sup> Calculated using Owens–Wendt's method [24].

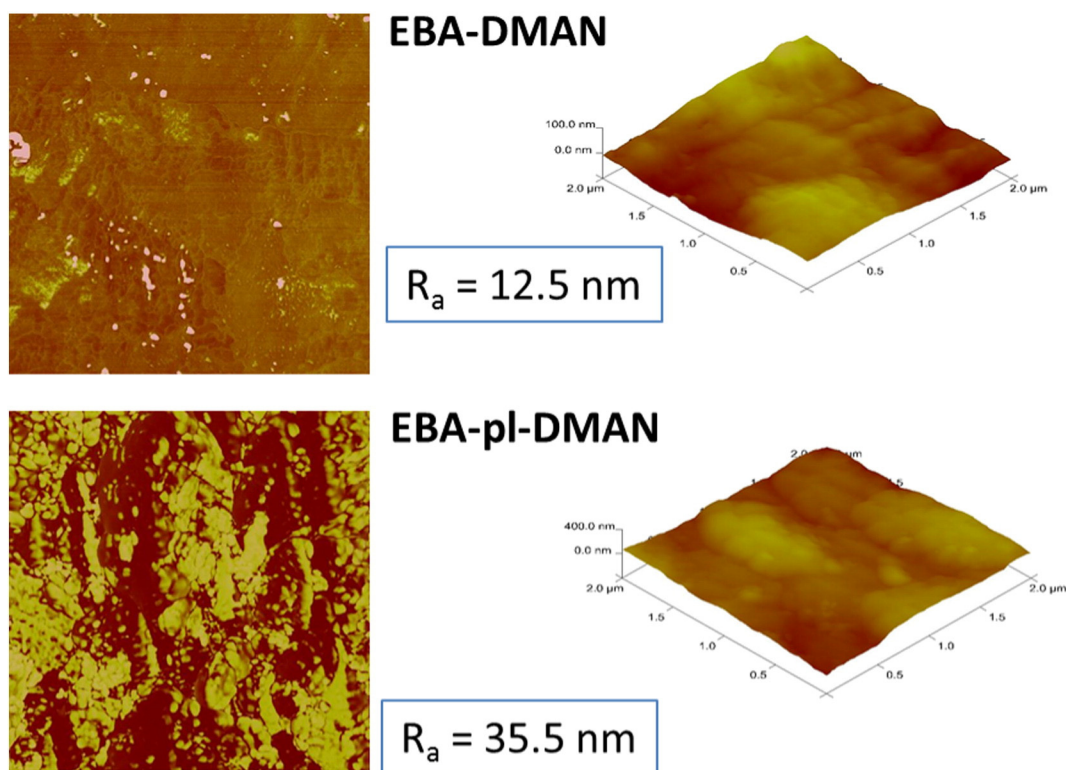


**Fig. 7.** AFM images and surface roughness ( $R_a$ ) of the modified polymer films: EBA-DMAN and oxygen plasma-treated EBA-pl-DMAN.

The surface-modified films with *N*-(2-hydroxyethyl)-4-dimethylamino-1,8-naphthalimide (EBA-DMAN) at a concentration of  $2.4 \pm 0.20 \mu\text{g cm}^{-2}$  determined by UV-spectroscopy exhibited properties as a reversible acidity sensor (until 4–5 cycles). The decrease in absorbance (ICT absorption band) and the corresponding quenching of

fluorescence because of the amine protonation of EBA-DMAN films occurs at lower pH values than that obtained for DMAN, and the solid sensor was used to evaluate the molarity of HCl solutions in the interval of 1–12 M.

Oxygen plasma treatment of the functionalized films increased appreciably the hydrophilic characteristic of the surface (EBA-pl-DMAN),

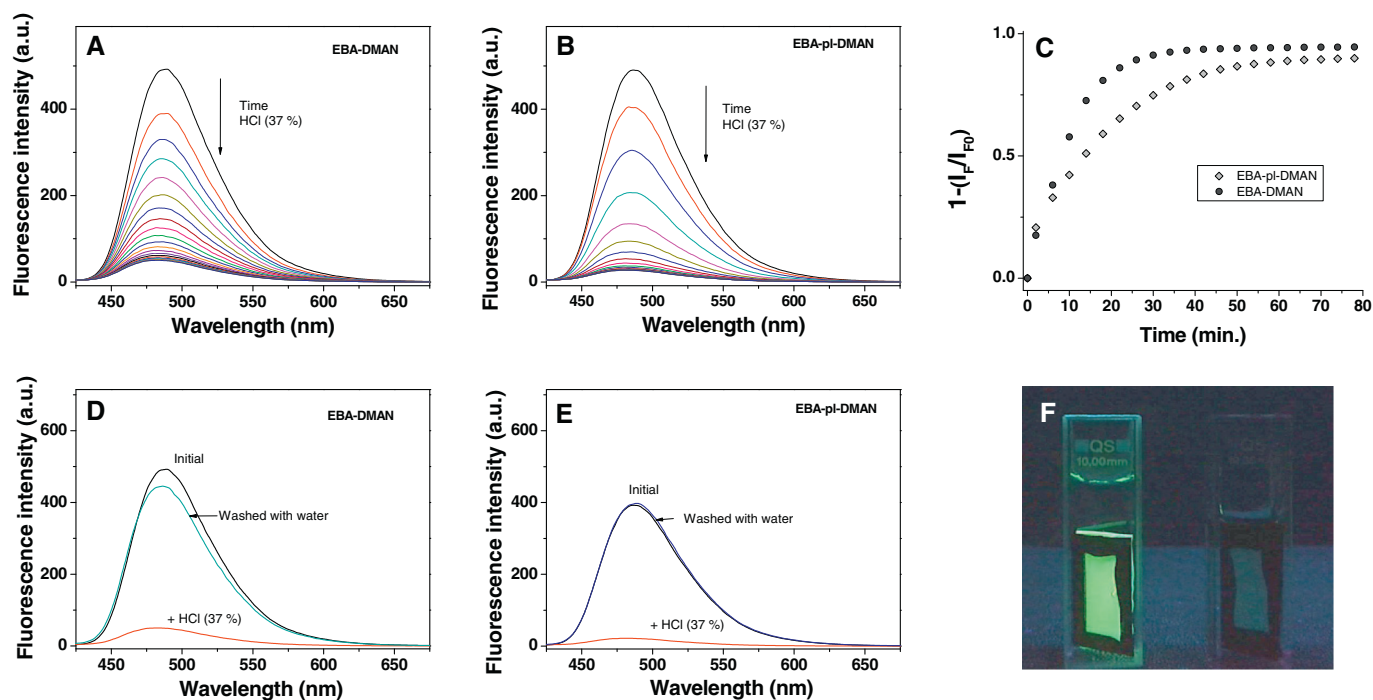


**Fig. 8.** Fluorescence decay with time for EBA-DMAN (A) and oxygen plasma-treated EBA-pl-DMAN (B) films using HCl (37% w/w, 12 M) aqueous solution. Response time comparison between both materials (C) and reversibility of dimethylamine protonation of the functionalized surfaces of EBA-DMAN (D) and EBA-pl-DMAN (E) after washing with distilled water and (F) fluorescence cells with EBA-pl-DMAN film, initial and after 30 min.



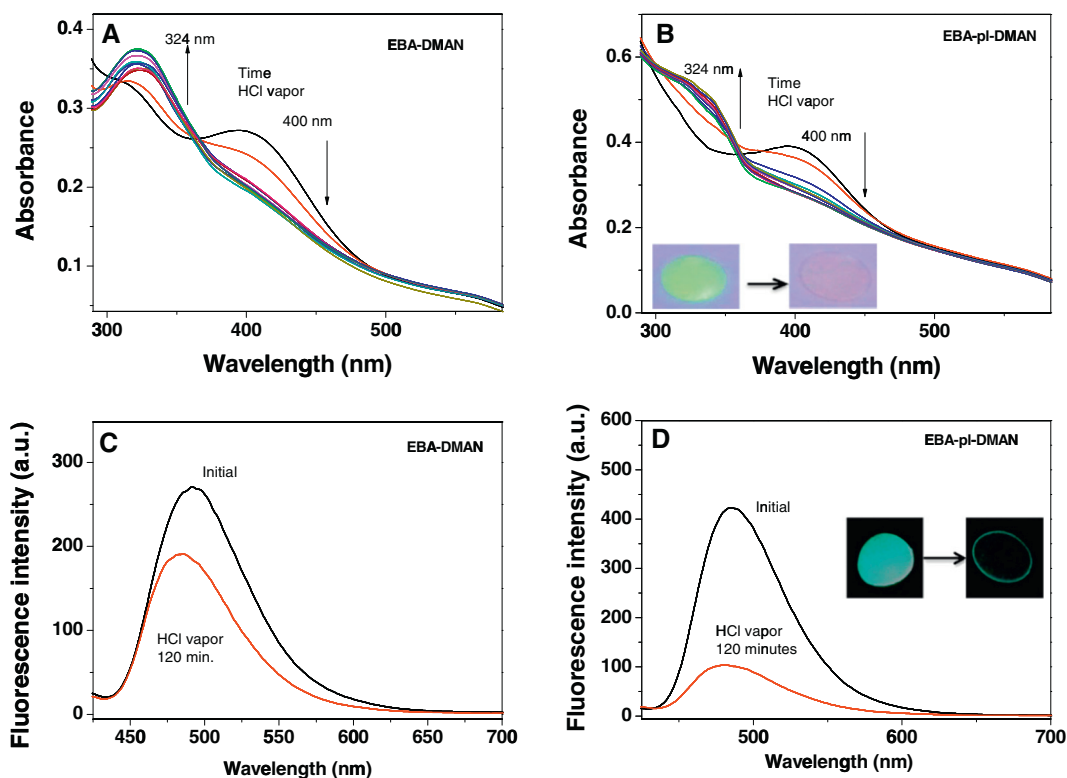


**Fig. 9.** Absorption changes with HCl vapors as a function of time (0–120 min) for functionalized films of EBA-DMAN (A) and EBA-pl-DMAN (B). Light blue fluorescence (488 nm) decreases after 120 min of vapors treatment for EBA-DMAN (C) and EBA-pl-DMAN (D). (For interpretation of the references to color in this figure legend, the reader is referred to the web version of this article.)

and the DMAN content bonded to the polymer remained constant after the treatment. The plasma treatment decreased the response time of the DMAN fluorescence to a strong acid medium (from 80 min for EBA-DMAN to 30 min for EBA-pl-DMAN in HCl, 12 M) and thus improved reversibility.

DMAN films bonded to the polymer were sensitive to the acid vapor medium, and the films treated with plasma (EBA-pl-DMAN) exhibited a better behavior in fluorescence decay, confirming that vapor penetration into the surface materials was improved by the surface oxidation induced by the plasma.

This new procedure using microwave reactions in a heterogeneous phase opens up the possibility to attach numerous interesting structures to polyolefin surfaces for application in materials of significant value such as environmental solid sensors.

## Acknowledgments

This study was supported by MINECO (Project Ref. MAT2012-31709). S. Fernández-Alonso thanks MINECO for a pre-doctoral fellowship linked to the project.

## References

- [1] L.S. Penn, H. Wang, *Polym. Advan. Technol.* 5 (1994) 809.
- [2] S.M. Desai, R.P. Singh, *Adv. Polym. Sci.* 169 (2004) 231.
- [3] L. López-Vilanova, I. Martínez, T. Corrales, F. Catalina, *React. Funct. Polym.* 85 (2014) 28.
- [4] V. Gaud, F. Rougé, Y. Gnanou, *React. Funct. Polym.* 72 (2012) 521.
- [5] M. Kondo, K. Goto, Y. Dozono, N. Kawatsuki, *React. Funct. Polym.* 73 (2013) 1567.
- [6] F. Cicogna, S. Coiai, C. Pinzino, F. Ciardelli, E. Passaglia, *React. Funct. Polym.* 72 (2012) 885.
- [7] I. Grabchev, R. Betcheva, *J. Photochem. Photobiol. A* 73 (2001) 142.
- [8] K. Wang, W. Huang, P. Xia, C. Gao, D. Yan, *React. Funct. Polym.* 52 (2002) 143.
- [9] E. Martin, R. Weigand, A. Pardo, *J. Lumin.* 68 (1996) 157.
- [10] W. Stewart, *J. Am. Chem. Soc.* 103 (1981) 7615.
- [11] S. Banerjee, E.B. Veale, C.M. Phelan, S.A. Murphy, G.M. Tocci, L.J. Gillespie, D.O. Frimannsson, J.M. Kelly, T. Gunnlaugsson, *Chem. Soc. Rev.* 42 (2013) 1601.

- [12] W. Zhu, C. Hu, K. Chen, H. Tian, *Synth. Met.* 96 (1998) 151.
- [13] H. Tian, J. Gan, K. Chen, J. He, Q. Song, X. Hou, *J. Mater. Chem.* 12 (2002) 1262.
- [14] I. Grabchev, J.M. Chovelon, *Polym. Adv. Technol.* 14 (2003) 601.
- [15] L. Jia, Y. Zhang, X. Guo, X. Qian, *Tetrahedron Lett.* 45 (2004) 3969.
- [16] W. Zhu, M. Hu, R. Yao, H. Tian, *J. Photochem. Photobiol. A* 154 (2003) 169.
- [17] I. Grabchev, I. Moneva, V. Bojinov, S. Guittouneau, *J. Mater. Chem.* 10 (2000) 1291.
- [18] I. Grabchev, J.M. Chovelon, X. Qian, *J. Photochem. Photobiol. A* 158 (2003) 37.
- [19] F. Cosnard, V. Wintgens, *Tetrahedron Lett.* 39 (1998) 2751.
- [20] P.L. Shuai Zheng, T.E.R. Mark Lynch, T.S. Moody, H.Q.N. Gunaratne, A.P. de Silva, *Photochem. Photobiol. Sci.* 11 (2012) 1675.
- [21] S. Hajatdoost, M. Olsthoorn, J. Yarwood, *Appl. Spectrosc.* 51 (1997) 1784.
- [22] P. Slepicka, Z. Malá, S. Rimpelova, N.S. Kasalkova, V. Svorcik, *React. Funct. Polym.* 95 (2015) 71.
- [23] G. Reynolds, K. Drexhage, *Opt. Commun.* 13 (1979) 222.
- [24] G.K. Owens, R.C. Wendt, *J. Appl. Polym. Sci.* 13 (1969) 1741.
- [25] H. Tian, J. Gan, K. Chen, J. He, Q.L. Song, X.Y. Hou, *J. Mater. Chem.* 12 (2002) 1262.
- [26] Y.Q. Tian, B.R. Shumway, C. Youngbull, A.K.Y. Jen, R.H. Johnson, D.R. Meldrum, *Sens. Actuators B Chem.* 147 (2010) 714.
- [27] Y.H. Cho, J.C. Park, *Tetrahedron Lett.* 38 (1997) 8331.
- [28] S. Rouhani, K. Ghraranjig, M.H. Nezhad, *Green Chem. Lett. Rev.* 7 (2014) 174.
- [29] A. Agarwal, P.M.S. Chauhan, *Synth. Commun.* 34 (2004) 2925.
- [30] Y. Wan, M. Alterman, M. Larhed, A. Hallberg, *J. Org. Chem.* 67 (2002) 6232.
- [31] A. Sharma, V.P. Mehta, E. Van der Eycken, *Tetrahedron* 64 (2008) 2605.
- [32] M. Tang, J. Hou, L. Lei, X. Liu, S. Guo, Z. Wang, K. Chen, *Int. J. Pharm.* 400 (2010) 66.
- [33] S. Hajatdoost, J. Yarwood, *J. Appl. Spectrosc.* 50 (1996) 558.
- [34] J. Sacristán, C. Mijangos, H. Reinecke, J. Spelle, J. Yarwood, *Macromolecular* 33 (2000) 6140.
- [35] J. Sacristán, H. Reinecke, C. Mijangos, S. Spell, J. Yarwood, *Macromol. Chem. Phys.* 203 (2002) 678.
- [36] M.S. Alexiou, V. Tychopoulos, S. Ghorbanian, J.H.P. Tymen, R.G. Brown, P.I. Brittain, *J. Chem. Soc. Perkin Trans. 2* (1990) 837.
- [37] P.A. Panchenko, O.A. Fedorova, Y.V. Fedorov, *Russ. Chem. Rev.* 82 (2014) 155.
- [38] K.A. Connors, *Binding Constants: The Measurement of Complex Stability*, Wiley, New York, 1987.
- [39] N. Slepíková Kasálková, P. Slepíčka, Z. Kolská, P. Sajdl, L. Bačáková, S. Rimpelová, V. Švorčík, *Nucl. Instrum. Meth. B* 272 (2012) 391.
- [40] P. Slepíčka, S. Trostová, N. Slepíková Kasálková, Z. Kolská, P. Sajdl, V. Švorčík, *Plasma Process. Polym.* 9 (2012) 197.
- [41] P. Slepíčka, N. Kasálková-Slepíčková, J. Siegel, Z. Kolská, L. Bačáková, V. Švorčík, *Bio-tech. Adv.* 33 (2015) 1120.
- [42] Y. Zheng, J. Miao, F. Zhang, C. Cai, A. Koh, T. Simmons, *React. Funct. Polym.* 100 (2016) 142.